

Stabilization of Complementarity Systems via Contact-Aware Controllers

Alp Aydinoglu¹, Victor M. Preciado¹, Michael Posa¹

Abstract—We propose a framework for provably stable local control of multi-contact robotic systems, directly utilizing force measurements and exploiting the complementarity structure of contact dynamics. Since many robotic tasks, like manipulation and locomotion, are fundamentally based in making and breaking contact with the environment, state-of-the-art control policies struggle to deal with the hybrid nature of multi-contact motion. Such controllers often rely heavily upon heuristics or, due to the combinatoric structure in the dynamics, are unsuitable for real-time control. Principled deployment of tactile sensors offers a promising mechanism for stable and robust control, but modern approaches often use this data in an ad hoc manner, for instance to guide guarded moves. In this work, we present a control framework which can close the loop on tactile sensors. Critically, this framework is non-combinatoric, enabling optimization algorithms to automatically synthesize provably stable control policies. We demonstrate this approach on multiple examples, including underactuated multi-contact problems, quasi-static friction problems and a high-dimensional problem with ten contacts.

Index Terms—Tactile feedback, optimization-based control, bilinear matrix inequalities, force control

I. INTRODUCTION

IN recent years, robotic automation has excelled in dealing with repetitive tasks in static and structured environments. On the other hand, to achieve the promise of the field, robots must perform efficiently in complex, unstructured environments which involve physical interaction between the robot and the environment itself. Furthermore, as compared with traditional motion planning problems, tasks like dexterous manipulation and legged locomotion fundamentally require intentionally initiating contact with the environment to achieve a positive result. To enable stable, and robust motion, it is critically important to design policies that explicitly consider the interaction between robot and environment.

Contact, however, is hybrid or multi-modal in nature, capturing the effect of stick-slip transitions or making and breaking contact. Standard approaches to control often match the hybrid dynamics with a hybrid or switching controller, where one policy is associated with each mode. However, precise identification of the hybrid events is difficult in practice, and switching controllers can be brittle, particularly local to the switching surface, or require significant hand-tuning. Model

predictive control, closely related to this work, is one approach that has been regularly applied to control through contact, with notable successes. Due to the computational complexity of hybrid model predictive control, these approaches must either approximate the hybrid dynamics [1], limit online control to a known mode sequence [2], are unable to perform in real time [3], or require large amount of samples [4]. While prior work has explored computational synthesis of non-switching feedback policies [5], it does not incorporate tactile sensing, and there are clear structural limits to smooth, state-based control. Here, we focus on offline synthesis of a stabilizing feedback policy, eliminating the need for intensive online calculations.

The need for contact-aware control is driven, in part, by recent advances in tactile sensing (e.g. [6], [7], [8], [9], [10] and others). Given these advances, there has been ongoing research to design control policies using tactile feedback for tasks that require making and breaking contact. However, these approaches are largely based on static assumptions, for instance with guarded moves [11], or rely upon switching controllers (e.g. [12], [13]). Other recent methods incorporate tactile sensors within deep learning frameworks, though offer no guarantees on performance or stability [14], [15].

In this work, we present an optimization-based numerical approach for designing control policies that use feedback on the contact forces. The control policy combines regular state feedback with tactile feedback in order to provably stabilize systems with possibly non-unique solutions. Our controller structure is non-combinatoric in nature and avoids enumerating the exponential number of potential hybrid modes that might arise from contact. More precisely, we design a controller where the contributions of each contact are additive, rather than combinatoric, in nature. Inspired by both prior work [5] and [16], we synthesize and verify a corresponding non-smooth, piecewise quadratic Lyapunov function. Furthermore, we also consider the scenario where there is a coupling between the contact force and the control loop such as friction models [17]. When these models are combined with tactile feedback controllers, they introduce an algebraic loop which we address by modeling actuator delay. Additionally, we are able to explicitly define sparsity patterns allowing us to design controllers for systems where the full state information might be lacking, such as when the state of an object is unknown but tactile information is available.

The primary contribution of this paper is an algorithm for synthesis of a control policy, utilizing state and force feedback, which is provably stabilizing even during contact mode transitions for systems with possibly non-unique solutions. To

*This work was supported by the National Science Foundation under Grant No. CMMI-1830218.

¹Alp Aydinoglu and Michael Posa are with the General Robotics, Automation, Sensing and Perception (GRASP) Laboratory, Victor M. Preciado is with the Department of Electrical and Systems Engineering, University of Pennsylvania, Philadelphia, PA 19104, USA. {alpayd, preciado, posa}@seas.upenn.edu (Corresponding author: Alp Aydinoglu)

achieve this, we choose a structure for controller and Lyapunov function designed specifically to leverage the complementarity structure of contact. While verification can be posed as a convex optimization problem, control synthesis is inherently harder. This problem is formulated and solved as a bilinear matrix inequality (BMI).

A preliminary version of this paper was presented at the International Conference on Robotics and Automation (ICRA) [18]. In this work, extensions are as follows.

- 1) The results are extended to a significantly broader class of systems.
 - The P-matrix assumption (Section II) is removed which enables design for systems with non-unique solutions (Section III).
 - Models where there is a coupling between the contact force and the control loop, including friction models are discussed (Section III).
 - Stability analysis (Section IV, Theorem 12) for this broader class of systems is presented.
- 2) Better approximations for the sets used in S-procedure (Section V, (13)) are introduced.
- 3) A polynomial optimization program (Section V, (23)) that can describe the non-unique solution sets of linear complementarity problems is introduced.
- 4) Four new examples are presented. Three of them are quasi-static friction models with non-unique contact forces. The fourth is a high dimensional example with eight states and ten contacts.

II. BACKGROUND

We first introduce the definitions and notation used throughout this work. For a positive integer l , \bar{l} denotes the set $\{1, 2, \dots, l\}$. Given a matrix $M \in \mathbb{R}^{k \times l}$ and two subsets $I \subseteq \bar{k}$ and $J \subseteq \bar{l}$, we define $M_{IJ} = (m_{ij})_{i \in I, j \in J}$. For two vectors $a \in \mathbb{R}^m$ and $b \in \mathbb{R}^m$, we use the notation $0 \leq a \perp b \geq 0$ to denote that $a \geq 0$, $b \geq 0$, $a^T b = 0$. The collection of all absolutely continuous functions on I is denoted as $AC(I)$. We denote the indeterminates as bold vectors, e.g. \mathbf{x} .

A. Linear Complementarity Systems

A standard approach to modeling robotic systems is through the framework of rigid-body systems with contacts. The continuous time dynamics can be modeled by the manipulator equations

$$M(q)\dot{v} + C(q, v) = Bu + J(q)^T \lambda, \quad (1)$$

where $q \in \mathbb{R}^p$ represents the generalized coordinates, $v \in \mathbb{R}^h$ represents the generalized velocities, $\lambda \in \mathbb{R}^m$ represents the contact forces, $M(q)$ is the inertia matrix, $C(q, v)$ represents the combined Coriolis and gravitational terms, B maps the control inputs $u \in \mathbb{R}^k$ into joint coordinates and $J(q)$ is the projection matrix (typically the contact Jacobian).

The model (1) is a hybrid dynamical system [19], [20] where the number of modes scale exponentially with m which arise from distinct combinations of contacts. One approach to

contact dynamics describes the forces using the complementarity framework where the generalized coordinates q and contact forces λ satisfy a set of complementarity constraints:

$$\lambda \geq 0, \phi(q, \lambda) \geq 0, \phi(q, \lambda)^T \lambda = 0, \quad (2)$$

where the function $\phi : \mathbb{R}^p \times \mathbb{R}^m \rightarrow \mathbb{R}^m$ is a gap function which relates the distance between robot and object with the contact force ([21], [22], [23] for more details). The complementarity framework is widespread within the robotics community and has been commonly used to simulate contact dynamics [24], [25], quasi-statics [17], leveraged in trajectory optimization [26], stability [27] and control [5] of rigid-body systems with contacts.

The local behavior of (1) with the constraints (2) can be captured by linear complementarity systems [28] [29]. A linear complementarity system is characterized by: $\bar{A} \in \mathbb{R}^{n_x \times n_x}$, $B \in \mathbb{R}^{n_x \times n_k}$, $\bar{D} \in \mathbb{R}^{n_x \times n_m}$, $a \in \mathbb{R}^{n_x}$, $\bar{E} \in \mathbb{R}^{n_m \times n_x}$, $\bar{F} \in \mathbb{R}^{n_m \times n_m}$, $H \in \mathbb{R}^{n_m \times n_k}$, $c \in \mathbb{R}^{n_m}$ in the following way:

Definition 1: (Linear Complementarity System) A linear complementarity system (LCS) describes the evolution of two time-dependent trajectories $\bar{x}(t) \in \mathbb{R}^{n_x}$ and $\lambda(t) \in \mathbb{R}^{n_m}$ for a given $u(t) \in \mathbb{R}^{n_k}$ and $x(0)$ such that

$$\begin{aligned} \dot{\bar{x}} &= \bar{A}\bar{x} + B u + \bar{D}\lambda + a, \\ 0 &\leq \lambda \perp \bar{E}\bar{x} + \bar{F}\lambda + H u + c \geq 0, \end{aligned} \quad (3)$$

where \bar{A} determines the autonomous dynamics of the state vector \bar{x} , B models the effect of the input on the state, \bar{D} describes the effect of the contact forces on the state and a models the constant forces acting on the state.

The matrices \bar{E}, \bar{F}, H^1 and the vector c capture the relationship between the contact force λ , the state vector \bar{x} and the input u . Note that the contact forces λ are always non-negative which holds for basic model of normal force and slack variables are typically used to represent sign-indefinite frictional forces. (3) implies that either $\lambda = 0$ or $\bar{E}\bar{x} + \bar{F}\lambda + H u + c = 0$, encoding the multi-modal dynamics of contact. Due to this complementarity structure, an LCS is a compact representation, as the variables and constraints scale linearly with m , rather than with the potential 2^m hybrid modes [30], [31].

B. Linear Complementarity Problem

A linear complementarity system is an ordinary differential equation (ODE) coupled with a variable that is the solution of a linear complementarity problem. Since linear complementarity problems play an important role in understanding and analyzing the LCS, we recall some definitions and results from the theory of linear complementarity problems [32].

Definition 2: (Linear Complementarity Problem) Given $F \in \mathbb{R}^{m \times m}$ and a vector $w \in \mathbb{R}^m$, the linear complementarity problem $LCP(w, F)$ is the following mathematical program:

$$\begin{aligned} \text{find} \quad & \lambda \in \mathbb{R}^m \\ \text{subject to} \quad & 0 \leq \lambda \perp F\lambda + w \geq 0. \end{aligned} \quad (4)$$

¹Even though the contact force λ does not depend on the input u in (2), local approximations of (1) and (2) can lead to models where the contact force depends on the input, e.g. [17], which is captured by the Hu term in the LCS (3).

For a given F and w , the LCP may have multiple solutions or none at all. Hence, we denote the solution set of the linear complementarity problem $\text{LCP}(w, F)$ as $\text{SOL}(w, F)$:

$$\text{SOL}(w, F) = \{\lambda : 0 \leq \lambda \perp F\lambda + w \geq 0\}.$$

In this work, we will consider LCP's where $\text{SOL}(w, F)$ can have more than one element for a given F and w . As a special case of this, we mention a particular class of LCP's that are guaranteed to have unique solutions.

Definition 3: (P-Matrix) A matrix $F \in \mathbb{R}^{m \times m}$ is a P-matrix, if the determinant of all of its principal sub-matrices are positive; that is, $\det(F_{\alpha\alpha}) > 0$ for all $\alpha \subseteq \{1, \dots, m\}$.

If F is a P-matrix, then the solution set $\text{SOL}(w, F)$ is a singleton for any $w \in \mathbb{R}^m$ [33]. If we denote the unique element of $\text{SOL}(w, F)$ as $\psi(w)$, then $\psi(w)$ is a piecewise linear function in $w \in \mathbb{R}^m$, hence is Lipschitz continuous and directionally differentiable.

If \bar{F} is a P-matrix, one can represent an LCS in a more compact manner. The linear complementarity system in (3) is equivalent to the dynamical system

$$\dot{\bar{x}} = A\bar{x} + Bu + D\lambda(\bar{x}, u), \quad (5)$$

where $\lambda(\bar{x}, u)$ corresponds to the unique element of $\text{SOL}(\bar{E}\bar{x} + Hu + c, \bar{F})$ for every state vector \bar{x} . Notice that (5) is only an alternative representation of (3) and still has the same structure as the LCS.

C. Sum-of-squares

In this work (Section V, (23)), describing the non-unique solution sets of LCP's is posed as a question of non-negativity of polynomials on basic semialgebraic sets. Towards this direction, we use the sum-of-squares (SOS) optimization.

A multivariate polynomial $p(x)$ is a sum-of-squares (SOS) if there exist polynomials $q_i(x)$ such that

$$p(x) = \sum_i q_i^2(x).$$

The existence of a sum-of-squares decomposition of a polynomial can be decided by solving a semidefinite programming feasibility problem [34], which is a convex optimization problem. We represent the semialgebraic conditions using the S-procedure technique [35], [36]. For example, to show that [37]

$$f(x) \geq 0, \quad \forall x \in \{z : g(z) \geq 0, h(z) = 0\},$$

it is sufficient to find polynomials $\sigma_1(x), \sigma_2(x), q(x)$ s.t.

$$\begin{aligned} \sigma_1(x)f(x) - \sigma_2(x)g(x) - q(x)h(x) &\geq 0, \\ \sigma_1(x) - 1 &\geq 0, \\ \sigma_2(x) &\geq 0. \end{aligned} \quad (6)$$

If constraints are in the form of (6) and the objective function is linear in the coefficients of any unknown/free polynomials, then the optimization problem can be represented as a semidefinite program (SDP) using the SOS relaxation.

III. LINEAR COMPLEMENTARITY SYSTEMS WITH TACTILE FEEDBACK

In this section, we present a tactile feedback controller where the input is dependent both on the state and the contact force ($u = u(x, \lambda)$), unlike the common approach of designing controllers only using the state feedback, ($u = u(x)$). Then, we describe the complementarity models with such tactile feedback controllers.

A. Tactile Feedback and Related Complementarity Models

We introduce the tactile feedback controller:

$$u(\bar{x}, \lambda) = K\bar{x} + L\lambda, \quad (7)$$

where $K \in \mathbb{R}^{n_k \times n_x}$ and $L \in \mathbb{R}^{n_k \times n_m}$. Using this control law, we will show that (3) can be transformed into the following LCS:

$$\begin{aligned} \dot{x} &= Ax + D\lambda + a, \\ 0 &\leq \lambda \perp Ex + F\lambda + c \geq 0, \end{aligned} \quad (8)$$

where $A \in \mathbb{R}^{n \times n}$, $D \in \mathbb{R}^{n \times m}$, $a \in \mathbb{R}^n$, $E \in \mathbb{R}^{m \times n}$, $F \in \mathbb{R}^{m \times m}$, $c \in \mathbb{R}^m$. If there is a coupling between the contact force and the control loop ($H \neq 0$), then we augment the state ($n > n_x$) to obtain (8). If there is no coupling, then $x = \bar{x}$ and $n = n_x$.

If the contact force does not depend on the input ($H = 0$), then application of the control law (7) trivially produces (8) with $A = \bar{A} + BK$, $D = \bar{D} + BL$, $E = \bar{E}$, and $F = \bar{F}$.

Next, we consider the case where the contact force depends on the input ($H \neq 0$). Since the input $u = u(\bar{x}, \lambda)$ similarly depends on the contact force, this introduces an algebraic loop. One might attempt to resolve this loop by simultaneously solving for both u and λ , leading to the closed-loop LCS:

$$\begin{aligned} \dot{x} &= (\bar{A} + BK)x + (\bar{D} + BL)\lambda + a, \\ 0 &\leq \lambda \perp Ex + F\lambda + c \geq 0, \end{aligned}$$

where $x = \bar{x}$, $E = \bar{E} + K$ and $F = \bar{F} + L$. Observe that the matrix F depends on the choice of the contact gain matrix L . Due to this dependency, the cardinality of the solution set $\text{SOL}(Ex + c, F)$ for a given x might change depending on the value of L . We demonstrate this with an example.

Example 4: Consider the complementarity constraint:

$$0 \leq \lambda \perp x + u + \lambda \geq 0,$$

where $x, u, \lambda \in \mathbb{R}$. If u is independent of λ , observe that $\text{SOL}(x + u, F)$ is a singleton for all pairs (x, u) since $F = [1]$ is a P-matrix. In this case, the contact force $\lambda_o(x, u)$ is equal to

$$\lambda_o(x, u) = \max\{0, -x - u\}.$$

However, for some choices of force-dependent inputs, this is no longer the case. From $u = L\lambda$, it follows that $F = [1 + L]$. For the case $L = -1$, the LCP for the closed-loop system is

$$0 \leq \lambda \perp x \geq 0.$$

The solution set is then:

$$\text{SOL}(x, F = 0) = \begin{cases} \{0\} & \text{if } x > 0, \\ [0, \infty) & \text{if } x = 0, \\ \emptyset & \text{if } x < 0. \end{cases}$$

We have infinitely many solutions for $x = 0$ and no solutions for $x < 0$.

Furthermore, resolving the algebraic loop by solving simultaneously for the contact force and the input is not physically realistic since control policies can not instantaneously respond to tactile measurements. As illustrated in Example 4, it is also mathematically problematic. Therefore, we will use the standard approach of modeling delay. Specifically, we model input delay using a low-pass filter:

$$\dot{\tau} = \kappa(u - \tau), \quad (9)$$

where $\kappa \in \mathbb{R}^+$ is the rate parameter. Using the low-pass filter model, we obtain the linear complementarity system:

$$\begin{aligned} \dot{\bar{x}} &= \bar{A}\bar{x} + B\tau + \bar{D}\lambda + a, \\ \dot{\tau} &= \kappa(u - \tau), \\ 0 &\leq \lambda \perp \bar{E}\bar{x} + F\lambda + H\tau + c \geq 0, \end{aligned} \quad (10)$$

Observe that the LCS model in (10) has the same form with (8) with the input (7):

$$\begin{aligned} \dot{x} &= \begin{bmatrix} \bar{A} & B \\ \kappa K & -\kappa I \end{bmatrix} x + \begin{bmatrix} \bar{D} \\ \kappa L \end{bmatrix} \lambda + \begin{bmatrix} a \\ 0 \end{bmatrix}, \\ 0 &\leq \lambda \perp \begin{bmatrix} \bar{E} & H \end{bmatrix} x + F\lambda + c \geq 0, \end{aligned}$$

where $x = [\bar{x}^T \ \tau^T]^T$. Observe that the delay decouples u and λ so the matrix F does not depend on the contact gain matrix L .

Alternatively, we note that one could add delay to the sensor dynamics:

$$\dot{\tau}_s = \kappa_s(\lambda - \tau_s).$$

While this approach would similarly resolve the algebraic loop, in this work we found out that modeling input delay produced better numerical results when combined with the algorithmic approach in Section V.

Using the control format in (7), for notational compactness, we will now exclusively consider closed-loop LCS in the form of (8).

B. Solution Concept

We introduce a solution concept for complementarity systems (1) and (8) similar to ([38], Definition 3.6).

Definition 5: A pair of functions $(x(t), \lambda(t))$ is a solution of the complementarity system,

$$\begin{aligned} \dot{x} &= f(x, \lambda), \\ 0 &\leq \lambda \perp \Phi(x, \lambda) \geq 0, \end{aligned}$$

where $f : \mathbb{R}^n \times \mathbb{R}^m \rightarrow \mathbb{R}^n$ and $\Phi : \mathbb{R}^n \times \mathbb{R}^m \rightarrow \mathbb{R}^m$ with the initial condition $x(0) = x_0$ if:

$$\begin{aligned} x(t) &\in AC([0, T]), \quad \forall T \geq 0, \\ \dot{x}(t) &= f(x(t), \lambda(t)) \text{ for almost all } t \in \mathbb{R}^+, \\ 0 &\leq \lambda(t) \perp \Phi(x(t), \lambda(t)) \geq 0 \text{ for almost all } t \in \mathbb{R}^+, \\ \lambda(t) &\text{ is almost everywhere differentiable.} \end{aligned}$$

It is important to note that since we take $x(t)$ to be absolutely continuous, we do not consider models where there are jumps (e.g. impact).

Proposition 6: If F in (8) is a P-matrix, then for every x_0 there exists a solution and it is unique.

Proof: Follows directly from ([16], Proposition 2.2) and Lipschitz continuity of $\lambda(x)$. ■

Note that if F is not a P-matrix, contact dynamics are known to generate non-unique solutions [39], [40]. In that case, one cannot guarantee the existence and uniqueness of solutions. Since the solutions are not unique, we denote the set of trajectories $x(t)$, with $t \geq t_0$, starting from x_0 as $\mathcal{S}(t_0, x_0)$ where the dependency on the LCS parameters is suppressed for ease of notation.

IV. STABILIZATION OF THE LINEAR COMPLEMENTARITY SYSTEM

In this section, we construct conditions for stabilization using non-smooth Lyapunov functions and contact-aware controllers.

We adopt notions of stability from [41]. If F is a P-matrix, these are equivalent to the notions of stability for differential equations where the right-hand side is Lipschitz continuous, though possibly non-smooth [16], [42].

Definition 7: The equilibrium x_e of LCS (8) is

- 1) stable in the sense of Lyapunov if, given any $\epsilon > 0$, there exists $\delta > 0$ such that

$$\|x_e - x_0\| < \delta \implies \|x(t) - x_e\| < \epsilon \quad \forall t \geq 0$$

for any x_0 and $x(t) \in \mathcal{S}(0, x_0)$.

- 2) asymptotically stable if it is stable and $\delta > 0$ exists s.t.

$$\|x_e - x_0\| < \delta \implies \lim_{t \rightarrow \infty} x(t) = x_e$$

for any x_0 and $x(t) \in \mathcal{S}(0, x_0)$.

A. Non-Smooth Lyapunov Function

In Lyapunov based analysis and synthesis methods, one desires to search over a wide class of functions. Here, we consider piecewise quadratic Lyapunov functions. They are more expressive than a Lyapunov function common to all modes (as was used in [5]), which makes it a more powerful choice than a single quadratic Lyapunov function [43]. Towards this direction, we consider a variant of the non-smooth Lyapunov function introduced in [16]:

$$V(x, \lambda) = x^T P x + 2x^T Q \lambda + \lambda^T R \lambda + p^T x + r^T \lambda + z, \quad (11)$$

where $P \in \mathbb{R}^{n \times n}$, $Q \in \mathbb{R}^{n \times m}$, $R \in \mathbb{R}^{m \times m}$, $p \in \mathbb{R}^n$, $r \in \mathbb{R}^m$, and $z \in \mathbb{R}$. The Lyapunov function (11) is quadratic in terms of the pair (x, λ) . If F is a P-matrix, it is piecewise quadratic in x since $\lambda = \lambda(x)$ is a piecewise affine function. For example, if all contact forces are inactive, $\lambda = 0$, then $V(x, \lambda(x)) = x^T P x + p^T x + z$. Even though V is non-smooth, it is locally Lipschitz continuous with respect to x if F is a P-matrix [16].

If F is not a P-matrix, then $\text{SOL}(Ex + c, F)$ is not a singleton and V becomes a set-valued function. Also, both $\lambda(t)$ and $V(x(t), \lambda(t))$ can be discontinuous due to the multi-valued nature of $\text{SOL}(Ex(t) + c, F)$. In the next example, we show that a discontinuous $V(x(t), \lambda(t))$ can be problematic.

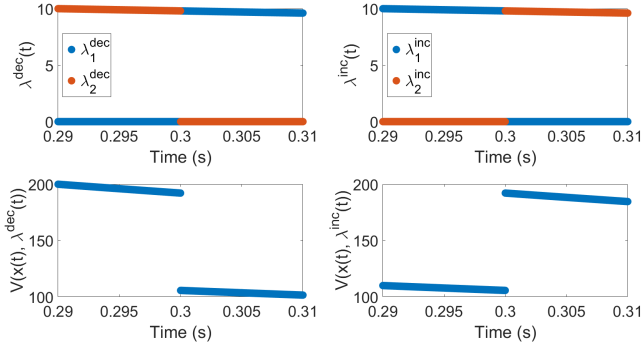


Fig. 1. Two different solutions for the set-valued Lyapunov function $V_s(x, \lambda) = x^2 + 0.1\lambda_1^2 + \lambda_2^2$.

Example 8: Consider the LCS:

$$\begin{aligned} \dot{x} &= -x + \lambda_1 + \lambda_2, \\ 0 &\leq \lambda_1 \perp x + \lambda_1 + \lambda_2 \geq 0, \\ 0 &\leq \lambda_2 \perp x + \lambda_1 + \lambda_2 \geq 0, \end{aligned}$$

where $x, \lambda_1, \lambda_2 \in \mathbb{R}$ and the set-valued Lyapunov function $V_s(x, \lambda) = x^2 + 0.1\lambda_1^2 + \lambda_2^2$. In Figure 1, we show the function's value for a solution $(x(t), \lambda^{\text{dec}}(t))$ where $\lambda^{\text{dec}}(t)$ jumps at $t = 0.3$ from λ_-^{dec} to λ_+^{dec} . Notice that the Lyapunov function also jumps at $t = 0.3$, decreasing. Then, we consider $\lambda^{\text{inc}}(t)$ that jumps at $t = 0.3$ where $\lambda_-^{\text{inc}} = \lambda_+^{\text{dec}}$ and $\lambda_+^{\text{inc}} = \lambda_-^{\text{dec}}$. The Lyapunov function increases for the solution $(x(t), \lambda^{\text{inc}}(t))$ as seen in Figure 1. Notice that $\lambda(t)$ can be discontinuous and jump in both directions. As this example illustrates, for any set-valued Lyapunov function that jumps negatively, there exists a solution such that the function jumps positively.

A set-valued Lyapunov function cannot decrease monotonically along all solutions as discussed in Example 8. For this reason, we focus on single-valued Lyapunov functions. Following the procedure in [16], one can parameterize Q , R and r such that $V(x, \lambda)$ is a single-valued function even when F is not a P-matrix. We introduce matrices W such that $WSOL(q, F)$ is a singleton for all q .

Proposition 9: ([16], Proposition 3.9) Assume that $WSOL(q, F)$ is a singleton for all q where $W \in \mathbb{R}^{n_w \times m}$. Then, the map $q \mapsto WSOL(q, F)$ is a continuous piecewise linear function of q .

The Lyapunov function (11) is single-valued if Q , R , r are such that $QSOL(Ex+c)$, $RSOL(Ex+c)$, and $r^T SOL(Ex+c)$ are singletons for all $x \in \mathbb{R}^n$. One can construct a Lyapunov function that is single-valued using a matrix W as in Proposition 9:

$$\begin{aligned} V(x, \lambda) &= x^T P x + 2x^T \tilde{Q} W \lambda + \lambda^T W^T \tilde{R} W \lambda \\ &\quad + p^T x + \sum_i \tilde{r}^T W \lambda + z, \end{aligned} \quad (12)$$

where $W \in \mathbb{R}^{n_w \times m}$, $\tilde{Q} \in \mathbb{R}^{n \times n_w}$, $\tilde{R} \in \mathbb{R}^{n_w \times n_w}$, $\tilde{r} \in \mathbb{R}^{n_w}$ and $WSOL(Ex+c, F)$ is a singleton. V is a non-smooth, continuous piecewise quadratic function in x and it is locally Lipschitz continuous.

Lemma 10: The Lyapunov function² $V(x, \lambda(x))$ as in (12) is locally Lipschitz continuous in x . Furthermore, $\bar{V}(t) = V(x(t), \lambda(t)) \in AC([0, T])$ for all $T \geq 0$ for the solutions as in Definition 5.

Proof: Since $W\lambda(x)$ is Lipschitz continuous in x , $V(x, \lambda(x))$ is locally Lipschitz continuous in x . Because $x(t)$ is absolutely continuous and $V(x, \lambda(x))$ is locally Lipschitz continuous, V is absolutely continuous in time. ■

From this point onward, without loss of generality, we use the Lyapunov function as defined in (12). Observe that if F is a P-matrix, we can trivially choose $W = I$. Furthermore, not all LCS where F is not a P-matrix admit useful W 's, but for many practical examples one can find such W 's. In Section V-B, we show how to generate W algorithmically.

Remark 11: Similar to the Lyapunov function, the input (7) is not necessarily continuous in time if F is not a P-matrix. If one desires a controller that is continuous in time, then the parametrization

$$u(\bar{x}, \lambda) = K\bar{x} + \tilde{L}W\lambda,$$

leads to a controller u that is continuous in time even if F is not a P-matrix. In this work, we consider the general input (7) that can be discontinuous. For most of the examples in Section VI, we use the parametrization $L = \tilde{L}W$ to ensure that the input is continuous in time which is desired in practice.

B. Conditions for Stabilization

Now, we construct conditions for stability in the sense of Lyapunov with the controller gains K and L as in (7), and the piecewise quadratic Lyapunov function V .

Theorem 12: Consider the linear complementarity system (8), and the Lyapunov function (12) with W such that $WSOL(Ex+c, F)$ is a singleton for all x . Assume there exists a solution for every x_0 and $x_e = 0$ is an equilibrium. If for all solutions $(x(t), \lambda(t))$ ³, there exists strictly positive constants γ_1, γ_2 , matrices K, L ⁴ and a function V such that

$$\gamma_1 \|x(t)\|_2^2 \leq V(x(t), \lambda(t)) \leq \gamma_2 \|x(t)\|_2^2,$$

and $\frac{d\bar{V}(t)}{dt} \leq 0$ for almost all t , then $x_e = 0$ is Lyapunov stable. Furthermore, if there exists a strictly positive constant γ_3 such that $\frac{d\bar{V}(t)}{dt} \leq -\gamma_3 \|x(t)\|_2^2$ for almost all t , then $x_e = 0$ is exponentially stable.

Proof: Let the solution $(x(t), \lambda(t))$ be arbitrary. Following Lemma 10, $\bar{V}(t)$ is absolutely continuous and almost everywhere differentiable on $[0, T]$ for all T . Then we have

$$\bar{V}(t) = \bar{V}(0) + \int_0^t \dot{\bar{V}}(s) ds \leq \bar{V}(0),$$

since $\dot{\bar{V}} \leq 0$ for almost all $t \in \mathbb{R}^+$. Since V is bounded and non-increasing, the rest follows from standard arguments for Lyapunov stability.

² $\lambda(x)$ is the set-valued function $\lambda(x) = SOL(Ex+c, F)$.

³Dependence on x_0 and LCS parameters is suppressed.

⁴ $\frac{d\bar{V}(t)}{dt}$ depends on K and L since \dot{x} is a function of K and L .

In order to prove exponential stability, observe that $\dot{V}(t) \leq -\gamma_3 \|x(t)\|_2^2$. Hence, it follows that

$$\|x(t)\|_2^2 \leq \frac{1}{\gamma_1} \bar{V}(0) - \frac{\gamma_3}{\gamma_1} \int_0^t \|x(s)\|_2^2 ds.$$

Using Gronwell's inequality, it follows that

$$\|x(t)\|_2^2 \leq \frac{1}{\gamma_1} \bar{V}(0) e^{-\frac{\gamma_3}{\gamma_1} t} \leq \frac{\gamma_2}{\gamma_1} \|x_0\|_2^2 e^{-\frac{\gamma_3}{\gamma_1} t}.$$

Hence we conclude that the equilibrium is exponentially stable. \blacksquare

We have established sufficient conditions to stabilize the LCS in (8). In Section V, we will show how Theorem 12 can be used to algorithmically synthesize a controller.

Observe that we assume existence of an upper-bound γ_2 in Theorem 12 since functions of the form (12) does not always have such upper-bounds, e.g. $z \neq 0$ and all other terms are zero. We observe that an upper-bound always exists under certain assumptions.

Remark 13: If $c \geq 0$, $a = 0$ and $z = 0$, there exists a γ_2 such that $V(x, \lambda) \leq \gamma_2 \|x\|_2^2$ since $W\lambda(x) \leq \rho \|x\|_2$ for all x for some ρ .

For this special case, an upper-bound always exists and one does not need to verify that V is upper-bounded when algorithmically synthesizing a controller (Section V).

V. CONTROLLER DESIGN AS A BILINEAR MATRIX INEQUALITY FEASIBILITY PROBLEM

In this section, we will describe how Theorem 12 can be used to algorithmically synthesize a controller. Then, we will propose a convex optimization program to find a matrix W such that $WSOL(Ex + c, F)$ is a singleton for all x . After that, we will turn the controller design problem into a bilinear matrix inequality (BMI) feasibility problem.

A. Stabilization of the Linear Complementarity System

The sufficient conditions in Theorems 12 are matrix inequalities that need to be satisfied for all solutions of the LCS (8). Now, we will transform them into matrix inequalities over two basic semialgebraic sets $\Gamma_{\text{SOL}}(E, F, c)$ and $\Gamma'_{\text{SOL}}(E, F, c)$.

We define the set $\Gamma_{\text{SOL}}(E, F, c)$:

$$\Gamma_{\text{SOL}}(E, F, c) = \{(\mathbf{x}, \boldsymbol{\lambda}) : 0 \leq \boldsymbol{\lambda} \perp E\mathbf{x} + c + F\boldsymbol{\lambda} \geq 0\},$$

where $(\mathbf{x}, \boldsymbol{\lambda}) \in \Gamma_{\text{SOL}}(E, F, c)$ are represented as quadratic inequalities. Similarly, we define the following set:

$$\begin{aligned} \Gamma'_{\text{SOL}}(E, F, c) = \{(\mathbf{x}, \boldsymbol{\lambda}, \boldsymbol{\lambda}') | \exists \boldsymbol{\rho}, \boldsymbol{\mu} : \boldsymbol{\lambda} \in \text{SOL}(E\mathbf{x} + c, F), \\ E\dot{\mathbf{x}} + F\boldsymbol{\lambda}' + \boldsymbol{\rho} = 0, \boldsymbol{\lambda}_i \boldsymbol{\rho}_i = 0, \boldsymbol{\lambda}'_i + \boldsymbol{\mu}_i = 0, \\ (E_i^T \mathbf{x} + F_i^T \boldsymbol{\lambda} + c_i) \boldsymbol{\mu}_i = 0, \boldsymbol{\mu}_i \boldsymbol{\rho}_i = 0\}, \end{aligned} \quad (13)$$

where $\dot{\mathbf{x}} = A\mathbf{x} + D\boldsymbol{\lambda} + a$ and $\boldsymbol{\mu}, \boldsymbol{\rho}$ are slack variables. Here $\boldsymbol{\lambda}'$ expresses the time derivative of the force.

Proposition 14: If the inequalities

$$\gamma_1 \|x\|_2^2 \leq V(\mathbf{x}, \boldsymbol{\lambda}) \leq \gamma_2 \|x\|_2^2, (\mathbf{x}, \boldsymbol{\lambda}) \in \Gamma_{\text{SOL}}, \quad (14)$$

$$\nabla_{\mathbf{x}} V(\mathbf{x}, \boldsymbol{\lambda})^T \dot{\mathbf{x}} + \nabla_{\boldsymbol{\lambda}} V(\mathbf{x}, \boldsymbol{\lambda})^T \boldsymbol{\lambda}' \leq 0, (\mathbf{x}, \boldsymbol{\lambda}, \boldsymbol{\lambda}') \in \Gamma'_{\text{SOL}}, \quad (15)$$

hold for the LCS (8) where $\dot{\mathbf{x}} = A\mathbf{x} + D\boldsymbol{\lambda} + a$, then the following inequalities hold for all solutions $(x(t), \lambda(t))$ of the LCS

$$\gamma_1 \|x(t)\|_2^2 \leq V(x(t), \lambda(t)) \leq \gamma_2 \|x(t)\|_2^2, \quad (16)$$

$$\frac{d}{dt} V(x(t), \lambda(t)) \leq 0, \quad (17)$$

for almost all $t \geq 0$.

Proof: Consider an arbitrary solution, $(x(t), \lambda(t))$ of (8). First we will show that (14) implies (16). From Definition 5, it follows that $\lambda(t) \in \text{SOL}(Ex + c, F)$ and $(x(t), \lambda(t)) \in \Gamma_{\text{SOL}}(E, F, c)$ for almost all $t \geq 0$. The result follows from (14).

Next, we show that (15) implies (17). We show that

$$\lambda(t) \in \text{SOL}(Ex(t) + c, F), \quad (18)$$

$$\lambda_i(t) > 0 \implies E_i^T \dot{x}(t) + F_i^T \lambda'(t) = 0, \quad (19)$$

$$E_i^T x(t) + F_i^T \lambda(t) + c_i > 0 \implies \lambda'_i(t) = 0, \quad (20)$$

$$\left. \begin{aligned} \lambda_i = 0 \\ E_i^T x + F_i^T \lambda + c = 0 \end{aligned} \right\} \implies \lambda'_i = 0 \text{ or } E_i^T \dot{x} + F_i^T \lambda' = 0, \quad (21)$$

hold for almost all $t \geq 0$ where dependency on t in (21) is suppressed for space limitations, $\lambda'(t) = \frac{d\lambda}{dt}$, and (18) directly follows from the definition of solution.

We define $n_i(t) = E_i^T x(t) + F_i^T \lambda(t) + c$ for notational simplicity. To prove (19)-(21), observe that for almost all $t \geq 0$, there exists an $\epsilon > 0$ such that both $\lambda_i(t)$ and $n_i(t)$ are continuous in the interval $[t - \epsilon, t + \epsilon]$. For almost all $t \geq 0$ if $\lambda_i(t) > 0$, then $n_i(t) = 0$ for a neighborhood around t hence $E_i^T \dot{x}(t) + F_i^T \lambda'(t) = 0$ and (19) follows. Similarly observe that if $n_i(t) > 0$, then $\lambda(t) = 0$ and $\lambda'(t) = 0$ as in (20). (21) follows from the fact that both $\lambda_i(t)$ and $n_i(t)$ cannot be positive at the same time.

Suppose (18)-(21) hold at some time t^* and consider $x_* = x(t^*)$, $\lambda_* = \lambda(t^*)$, $\lambda'_* = \lambda'(t^*)$ and $\dot{x}_* = \dot{x}(t^*)$. We will show that $(x_*, \lambda_*, \lambda'_*) \in \Gamma'_{\text{SOL}}(E, F, c)$.

There are 3 cases. First consider the case where $\lambda_{i,*} > 0$ and therefore $(E_i^T x_* + F_i^T \lambda_* + c_i) = 0$. Observe that all equalities in (13) are satisfied with $\rho_{i,*} = 0$ and $\mu_{i,*} = -\lambda'_{i,*}$.

For the case where $\lambda_{i,*} = 0$ and $(E_i^T x_* + F_i^T \lambda_* + c_i) > 0$, all equalities are satisfied with $\rho_{i,*} = -E_i^T \dot{x}_* - F_i^T \lambda'_{i,*}$ and $\mu_{i,*} = 0$.

For the last case where both $(E_i^T x_* + F_i^T \lambda_* + c_i) = \lambda_{i,*} = 0$, the equalities are satisfied with either $\rho_{i,*} = 0$, $\mu_{i,*} = -\lambda'_{i,*}$ or $\rho_{i,*} = -E_i^T \dot{x}_* - F_i^T \lambda'_{i,*}$, $\mu_{i,*} = 0$.

Since the implications hold for almost all t , we conclude that $(x(t), \lambda(t), \lambda'(t)) \in \Gamma'_{\text{SOL}}$ for almost all $t \geq 0$. The result follows from (15). \blacksquare

Following Proposition 14 and Theorem 12, if the matrix inequalities over basic semialgebraic sets (14), (15) are satisfied, one can conclude that the equilibrium x_e is Lyapunov stable. Similarly, one can show that the equilibrium is exponentially stable if left side of (15) is upper-bounded by $-\gamma_3 \|x\|_2^2$ as in Theorem 12.

B. Computing W via Polynomial Optimization

Until this point, we have assumed that we have access to a W such that $WSOL(Ex + c, F)$ is a singleton for all

$x \in \mathbb{R}^n$. If F is a P-matrix, one can always pick $W = I$ since $\text{SOL}(Ex + c, F)$ is a singleton for any x as discussed earlier. For the non-P case, one can always trivially pick $W = 0$ which turns the Lyapunov function (12) into a common Lyapunov function. On the other hand, it is clearly better to search over a wider range of Lyapunov functions and not restrict ourselves to the common Lyapunov function [43], [16]. Hence we want to maximize the rank of W . More precisely, we want to solve the following optimization problem:

$$\begin{aligned} & \max_W \quad \text{rank}(W) \\ & \text{subject to} \quad \text{WSOL}(q, F) \text{ is a singleton for all } q. \end{aligned}$$

To solve this problem, we propose an algorithm based in a sequence of convex optimization problems.

Proposition 15: Suppose the following inequalities hold for all q , all $\lambda_{1,q}, \lambda_{2,q} \in \text{SOL}(q, F)$ and some vector w :

$$\begin{aligned} (\eta + w^T(\lambda_{1,q} - \lambda_{2,q}))(\lambda_{1,q}^T \lambda_{1,q} + \lambda_{2,q}^T \lambda_{2,q}) &\geq 0, \\ (\eta - w^T(\lambda_{1,q} - \lambda_{2,q}))(\lambda_{1,q}^T \lambda_{1,q} + \lambda_{2,q}^T \lambda_{2,q}) &\geq 0. \end{aligned} \quad (22)$$

where $\eta > 0$ is a constant slack parameter. Then, $w^T \text{SOL}(q, F)$ is a singleton for all q .

Proof: Observe that

$$\lambda \in \text{SOL}(q, F) \implies \alpha \lambda \in \text{SOL}(\alpha q, F),$$

for all $\alpha \geq 0$. We will show that the positive homogeneity property leads to:

$$|w^T(\lambda_{1,q} - \lambda_{2,q})| \leq \eta \forall q \implies |w^T(\lambda_{1,q} - \lambda_{2,q})| = 0 \forall q.$$

Assume that there exists $\eta^* > 0$ such that $|w^T(\lambda_{1,q^*} - \lambda_{2,q^*})| = \eta^*$ for some q^* . Pick $\alpha^* > 0$ such that $\alpha^* \eta^* > \eta$ and $|w^T(\alpha^* \lambda_{1,q^*} - \alpha^* \lambda_{2,q^*})| = \alpha^* \eta^* > \eta$. Due to the positive homogeneity property, there exists $\lambda_{1,\alpha q^*}$ and $\lambda_{2,\alpha q^*}$ such that $|w^T(\lambda_{1,\alpha q^*} - \lambda_{2,\alpha q^*})| = \alpha^* \eta^* > \eta$. This leads to a contradiction.

Next, we consider q such that $(\lambda_{1,q}^T \lambda_{1,q} + \lambda_{2,q}^T \lambda_{2,q}) > 0$. It follows from (22) that $|w^T(\lambda_{1,q} - \lambda_{2,q})| \leq \eta$ hence $|w^T(\lambda_{1,q} - \lambda_{2,q})| = 0$. If $(\lambda_{1,q}^T \lambda_{1,q} + \lambda_{2,q}^T \lambda_{2,q}) = 0$, then $\lambda_{1,q} = \lambda_{2,q} = 0$ and it trivially holds that $w^T \lambda_{1,q} = w^T \lambda_{2,q}$. Therefore, for any w such that (22) holds, $w^T \lambda_{1,q} = w^T \lambda_{2,q}$ also holds for all q . Hence, $w^T \text{SOL}(q, F)$ is a singleton for all q . ■

Given a matrix $W_d \in \mathbb{R}^{s \times m}$, one can utilize Proposition 15 in order to find a vector w such that $w^T \text{SOL}(q, F)$ is a singleton (for all q) and w^T is linearly independent with the rows of W_d . Consider the optimization problem:

$$\begin{aligned} & \min_{w, \eta} \quad r^T N^T w \quad (23) \\ & \text{subject to} \quad (\eta + w^T(\lambda_1 - \lambda_2))(\lambda_1^T \lambda_1 + \lambda_2^T \lambda_2) \geq 0, \\ & \quad (\eta - w^T(\lambda_1 - \lambda_2))(\lambda_1^T \lambda_1 + \lambda_2^T \lambda_2) \geq 0, \\ & \quad \text{for } \lambda_1, \lambda_2 \in \text{SOL}(q, F), \\ & \quad |w_i| \leq 1, \forall i, \eta \geq 0, \end{aligned}$$

where r is a random vector with entries sampled from uniform distribution ($r_i \sim U(0, 1)$), N is a basis for the nullspace of W_d ($\mathcal{N}(W_d)$), λ_1, λ_2, q are indeterminates, and the set inclusion is incorporated via the S-procedure for the first two inequalities.

Algorithm 1 Find W

Require: F

```

Initialization :  $N \leftarrow I, W = []$ 
1: while  $\min r^T N^T w \neq 0$  do
2:    $r_i \sim U(0, 1)$  (for each element of  $r$ )
3:   Solve (23) and obtain  $w$ 
4:   if  $\min r^T N^T w < 0$  then
5:      $W \leftarrow \begin{bmatrix} W \\ w^T \end{bmatrix}$ 
6:   Calculate  $N$  based on  $\mathcal{N}(W)$ 
7:   end if
8: end while
9: return  $W$ 

```

Proposition 16: Consider W_d and the optimization (23). If there exists a w such that the constraints hold, and w^T is linearly independent with the rows of W_d , then $\min r^T N^T w < 0$ almost surely.

Proof: Assume there exists a w that is feasible for optimization problem (23) and w^T is linearly independent with the rows of W_d . Then, $\|N^T w\| > 0$ and $r^T N^T w \neq 0$ with probability 1. By homogeneity, an optimal w_* can be found such that $r^T N^T w_* < 0$. ■

We now introduce Algorithm 1 based on Proposition 16. The algorithm almost surely finds a new linearly independent vector that satisfies the constraints in (23) if it exists and terminates when there are not any left.

During our computational experiments, the slack parameter η played an important role in solving the polynomial optimization problem (23) and the solvers (Mosek [44], SeDuMi [45]) had trouble verifying the status of the problem (feasible or infeasible) when $\eta = 0$.

C. Control Design

Since we have defined the sets $\Gamma_{\text{SOL}}(E, F, c)$, $\Gamma'_{\text{SOL}}(E, F, c)$ and described a procedure to find a matrix W , we can formulate the feasibility problem with strictly positive constants γ_1, γ_2 and non-negative γ_3 :

$$\text{find } V(\mathbf{x}, \boldsymbol{\lambda}), K, L \quad (24)$$

$$\begin{aligned} \text{s.t. } & \gamma_1 \|\mathbf{x}\|_2^2 \leq V(\mathbf{x}, \boldsymbol{\lambda}) \leq \gamma_2 \|\mathbf{x}\|_2^2, (\mathbf{x}, \boldsymbol{\lambda}) \in \Gamma_{\text{SOL}}(E, F, c), \\ & \frac{dV}{dt} \leq -\gamma_3 \|\mathbf{x}\|_2^2, (\mathbf{x}, \boldsymbol{\lambda}, \boldsymbol{\lambda}') \in \Gamma'_{\text{SOL}}(E, F, c), \end{aligned}$$

with the function $V(\mathbf{x}, \boldsymbol{\lambda})$ as in (12) and

$$\begin{aligned} \frac{dV}{dt} &= 2\mathbf{x}^T P(A\mathbf{x} + D\boldsymbol{\lambda} + a) + 2(A\mathbf{x} + D\boldsymbol{\lambda} + a)^T \tilde{Q}W\boldsymbol{\lambda} \\ &\quad + 2\mathbf{x}^T \tilde{Q}W\boldsymbol{\lambda}' + 2\boldsymbol{\lambda}^T W^T \tilde{R}W\boldsymbol{\lambda}' + p^T \dot{\mathbf{x}} + \tilde{r}W_i^T \boldsymbol{\lambda}'. \end{aligned}$$

Here, V encodes the non-smoothness of the problem structure, mirroring the structure of the LCS, and allow tactile feedback design without exponential enumeration. This is an appealing middle ground between the common Lyapunov function of our prior work [5], and purely hybrid approaches [46], [47]. We can assign a different Lyapunov function and a control policy for each mode but avoid mode enumeration so the approach can scale to large number of contacts m .

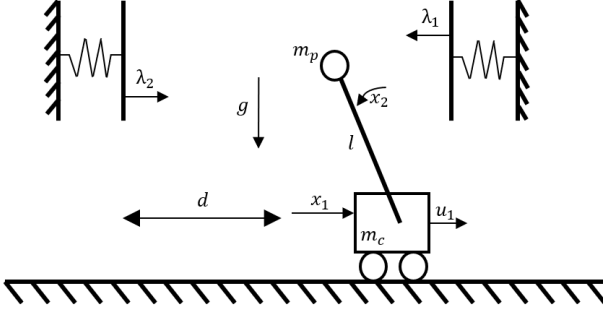


Fig. 2. Benchmark problem: Regulation of the cart-pole system to the origin with soft walls.

Notice that the inequality with $\frac{dV}{dt}$ is a bilinear matrix inequality because of the bilinear terms such as PA where A depends on the gain matrix K as discussed in Section III. In (24), we have formulated the problem of designing a control policy as finding a feasible solution for a set of bilinear matrix inequalities. The sets $\Gamma_{\text{SOL}}(E, F, c)$ and $\Gamma'_{\text{SOL}}(E, F, c)$ are incorporated via the S-procedure.

VI. EXAMPLES

In this paper, we use the YALMIP [48] toolbox with PENBMI [49] to formulate and solve bilinear matrix inequalities. SeDuMi [45] and Mosek [44] are used for solving the semidefinite programs (SDP's). PATH [50] has been used to solve the linear complementarity problems when performing simulations. The code for all examples is available⁵ and examples are provided with a video depiction⁶. The experiments are done on a desktop computer with the processor *Intel i7-9700* and *16GB RAM*.

A. Cart-Pole with Soft Walls

We consider the cart-pole system where the goal is to balance the pole and regulate the cart to the center, where there are frictionless walls, modeled via spring contacts, on both sides. This problem, or a slight variation of it, has been used as a benchmark in control through contact [47], [51], [3] and the model is shown in Figure 2.

In our model, the x_1 is the position of the cart, x_2 is the angle of the pole, and x_3, x_4 are their respective time derivatives. The input u_1 is a force applied to the cart, and the contact forces of the walls are represented with λ_1 and λ_2 , leading to the LCS

$$\begin{aligned}\dot{x}_1 &= x_3, \\ \dot{x}_2 &= x_4, \\ \dot{x}_3 &= \frac{gm_p}{m_c} x_2 + \frac{1}{m_c} u_1, \\ \dot{x}_4 &= \frac{g(m_c + m_p)}{lm_c} x_2 + \frac{1}{lm_c} u_1 + \frac{1}{lm_p} \lambda_1 - \frac{1}{lm_p} \lambda_2,\end{aligned}$$

⁵ <https://github.com/AlpAydinoglu/cdesign>

⁶ <https://www.youtube.com/watch?v=17SyKMCaINg>

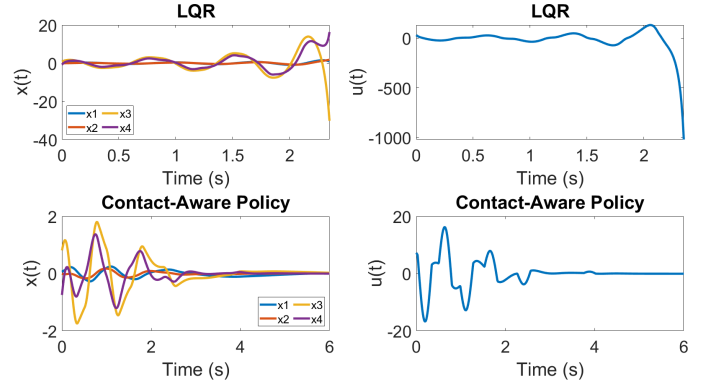


Fig. 3. Performance of LQR and contact-aware policy starting from the same initial condition for the cart-pole with soft walls example. LQR is unstable whereas contact-aware policy is successful.

$$\begin{aligned}0 &\leq \lambda_1 \perp lx_2 - x_1 + \frac{1}{k_1} \lambda_1 + d \geq 0, \\ 0 &\leq \lambda_2 \perp x_1 - lx_2 + \frac{1}{k_2} \lambda_2 + d \geq 0,\end{aligned}$$

where $k_1 = k_2 = 10$ are stiffness parameters of the soft walls, $g = 9.81$ is the gravitational acceleration, $m_p = 0.1$ is the mass of the pole, $m_c = 1$ is the mass of the cart, $l = 0.5$ is the length of the pole, and $d = 0.1$ represents where the walls are. For this model, we solve the feasibility problem (24) and find a controller of the form $u(x, \lambda) = Kx + L\lambda$ that regulates the model to the origin. The algorithm succeeded in finding a feasible controller in 0.72 seconds. As a comparison, we also designed an LQR controller with penalty on the state $Q = 10I$ and penalty on the input $R = 1$. We tested both contact-aware and LQR controllers on the nonlinear plant for 100 initial conditions where $x_2(0) = 0$, and $x_1(0), x_3(0), x_4(0)$ are uniformly distributed ($10x_1(0), x_3(0), x_4(0) \sim U[-1, 1]$). Despite the fact that the walls are not particularly stiff, LQR was successful only 71% of the time, whereas our contact-aware policy was always successful. In Figure 3, we present an example where both LQR and contact-aware policy start from the same initial conditions and LQR fails whereas our policy is successful.

B. Partial State Feedback

We consider a model that consists of three carts on a frictionless surface as in Figure 4. The cart on the left is

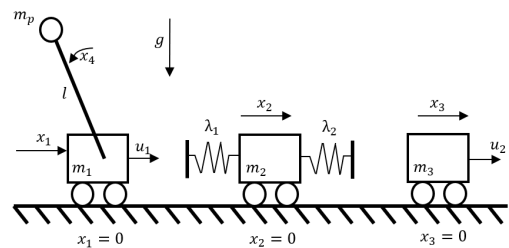


Fig. 4. Regulation of carts to their respective origins without observation of the middle cart.

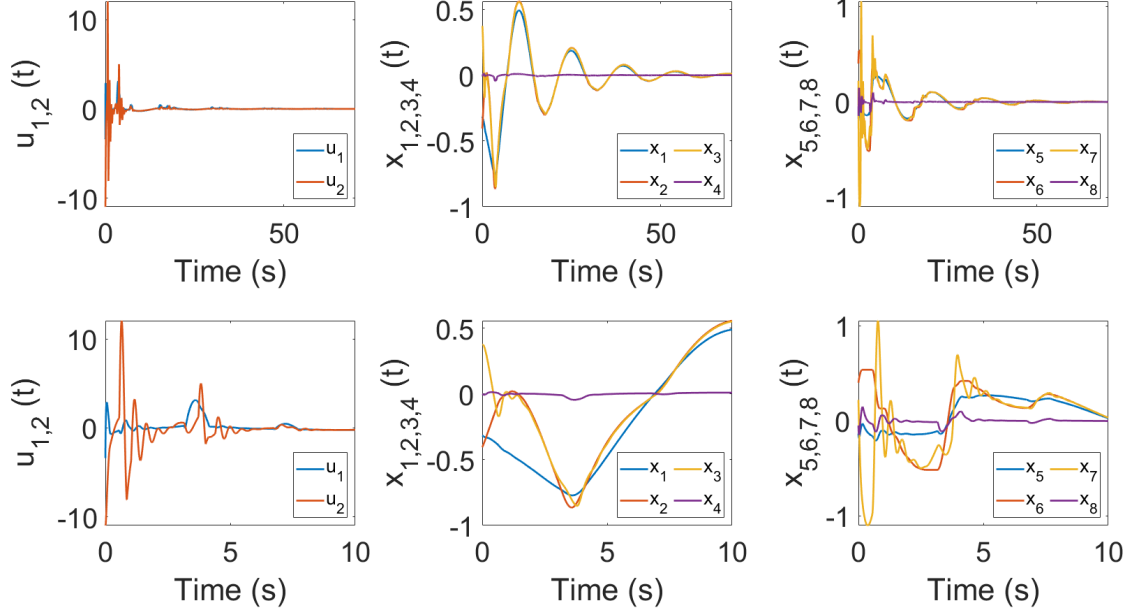


Fig. 5. Simulation with contact-aware policy for partial state-feedback example. The plots on the top row show the input and the state variables ($u(t), x(t)$) for the time interval $t = [0, 60]$. Second row demonstrates the time interval $t = [0, 10]$ for the same initial condition.

attached to a pole and the cart in the middle makes contact via soft springs. In this model, a spring only becomes active if the distance between the outer block and the block in the middle is less than some threshold. Here, x_1, x_2, x_3 represent the positions of the carts and x_4 is the angle of the pole. The corresponding LCS is

$$\begin{aligned} \ddot{x}_1 &= \frac{gm_p}{m_1}x_4 + \frac{1}{m_1}u_1 - \frac{1}{m_1}\lambda_1, \\ \ddot{x}_2 &= \frac{\lambda_1}{m_2} - \frac{\lambda_2}{m_2}, \\ \ddot{x}_3 &= \frac{\lambda_2}{m_3} + \frac{u_2}{m_3}, \\ \ddot{x}_4 &= \frac{g(m_1 + m_p)}{m_1l}x_4 + \frac{u_1}{m_1l} - \frac{1}{m_1l}\lambda_1, \\ 0 &\leq \lambda_1 \perp x_2 - x_1 + \frac{1}{k_1}\lambda_1 \geq 0, \\ 0 &\leq \lambda_2 \perp x_3 - x_2 + \frac{1}{k_2}\lambda_2 \geq 0, \end{aligned}$$

where the masses of the carts are $m_1 = m_2 = m_3 = 1$, $g = 9.81$ is the gravitational acceleration, $m_p = 1.5$ is the mass of the pole, $l = 0.5$ is the length of the pole, and $k_1 = k_2 = 20$ are stiffness parameters of the springs. Observe that we have control over the outer blocks, but do not have any control over the block in the middle. Additionally, we assume that we cannot observe the middle block, and can only observe the outer blocks and the contact forces. For this example, we can solve the feasibility problem (24) in 9.3 seconds and find a controller of the form $u(x, \lambda) = Kx + L\lambda$. We enforce sparsity on the controller K and do not use any feedback from the state x_2 or its derivative \dot{x}_2 . This example demonstrates that tactile feedback can be used in scenarios where full state information

is lacking. In Figure 5, we demonstrate the performance of the controller.

C. Acrobot with Soft Joint Limits

As a third example, we consider the classical underactuated acrobot, a double pendulum with a single actuator at the elbow (see [52] for the details of the acrobot dynamics). Additionally, we add soft joint limits to the model. Hence we consider the model in Figure 6:

$$\dot{x} = Ax + Bu + D\lambda,$$

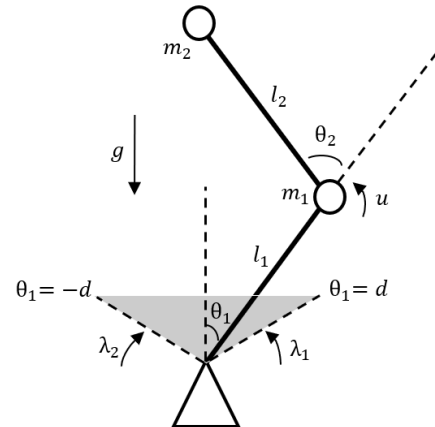


Fig. 6. Acrobot with soft joint limits.

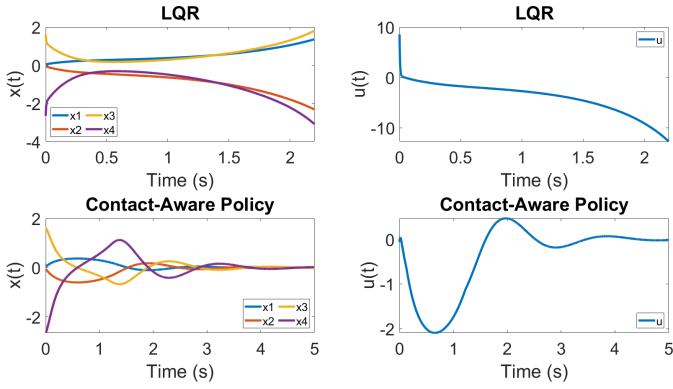


Fig. 7. Simulation of LQR and contact-aware policy starting from the same initial condition for the acrobot with soft joint limits example. LQR is unstable whereas contact-aware policy is successful.

where $x = (\theta_1, \theta_2, \dot{\theta}_1, \dot{\theta}_2)$, $\lambda = (\lambda_1, \lambda_2)$, and $D = \begin{bmatrix} 0_{2 \times 2} \\ M^{-1} J^T \end{bmatrix}$

with $J^T = \begin{bmatrix} -1 & 1 \\ 0 & 0 \end{bmatrix}$. For this model, the masses of the rods are $m_1 = 0.5$, $m_2 = 1$, the lengths of the rods are $l_1 = 0.5$, $l_2 = 1$, and the gravitational acceleration is $g = 9.81$. We model the soft joint limits using the following complementarity constraints:

$$\begin{aligned} 0 \leq d - \theta_1 + \frac{1}{k} \lambda_1 \perp \lambda_1 &\geq 0, \\ 0 \leq \theta_1 + d + \frac{1}{k} \lambda_2 \perp \lambda_2 &\geq 0, \end{aligned}$$

where $k = 1$ is the stiffness parameter and $d = 0.2$ is the angle that represents the joint limits in terms of the angle θ_1 . For this example, we solve the feasibility problem (24) and obtain a controller of the form $u(x, \lambda) = Kx + L\lambda$ in 1.18 seconds. For comparison, we also designed an LQR controller for the linear system where the penalty on the state is $Q = 100I$ and the penalty on the input is $R = 1$. We ran 100 trials on the nonlinear plant where initial conditions were sampled according to $x_1(0) = x_2(0) = 0$ and $x_3(0), x_4(0) \sim U[-0.05, 0.05]$. Out of these 100 trials, LQR was successful only 49% of the time whereas our design was successful 87% of the time. In Figure 7, we present a case where LQR fails and contact-aware policy is successful.

D. Box with Friction

We consider a quasi-static model of a box on a surface, as in Figure 8, where μ is the coefficient of friction between the box and the ground. We approximate Newton's second law with a force balance equation with Coulomb friction and damping. The goal is to regulate the box to the center. This simple model serves as an example where F is not a P-matrix and the complementarity constraints have a dependency on the input u ($H \neq 0$). Here, x is the position of the box, u is the input, λ_+ is the positive component of the friction force, λ_-

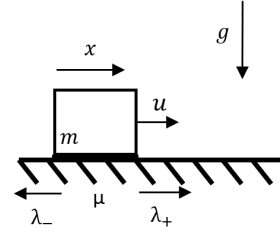


Fig. 8. Regulation task of a box standing on a surface with Coulomb friction.

is the negative component of the friction force and γ is the slack variable:

$$\begin{aligned} \alpha \dot{x} &= u + \lambda_+ - \lambda_-, \\ 0 \leq \gamma \perp \mu mg - \lambda_+ - \lambda_- &\geq 0, \\ 0 \leq \lambda_+ \perp \gamma + u + \lambda_+ - \lambda_- &\geq 0, \\ 0 \leq \lambda_- \perp \gamma - u - \lambda_+ + \lambda_- &\geq 0, \end{aligned}$$

where $m = 1$ is the mass of the box, $g = 9.81$ is the gravitational acceleration $\mu = 0.1$ is the friction coefficient, and $\alpha = 4$ is the damping coefficient. We model the input delay with the low-pass filter model and obtain:

$$\begin{aligned} \alpha \dot{x} &= \tau + \lambda_+ - \lambda_-, \\ \dot{\tau} &= \kappa(u - \tau), \\ 0 \leq \gamma \perp \mu mg - \lambda_+ - \lambda_- &\geq 0, \\ 0 \leq \lambda_t^+ \perp \gamma + \tau + \lambda_+ - \lambda_- &\geq 0, \\ 0 \leq \lambda_t^- \perp \gamma - \tau - \lambda_+ + \lambda_- &\geq 0, \end{aligned}$$

where $\kappa = 100$. Since F is not a P-matrix, we use Algorithm 1 and find $W = [0 \ 1 \ -1]$ such that $WSOL(q, F)$ is a singleton for all q . For this example, W shows that the net friction force, $\lambda_+ - \lambda_-$ is always unique. Notice that the x -trajectory, $x(t)$ is unique, but the λ -trajectory, $\lambda(t)$ is not. We can solve the feasibility problem in (24) in 22 seconds and find a controller of the form $u(x, \lambda) = Kx + \tilde{L}W\lambda$ such that the system is Lyapunov stable. In Figure 9, we demonstrate the performance of the controller.

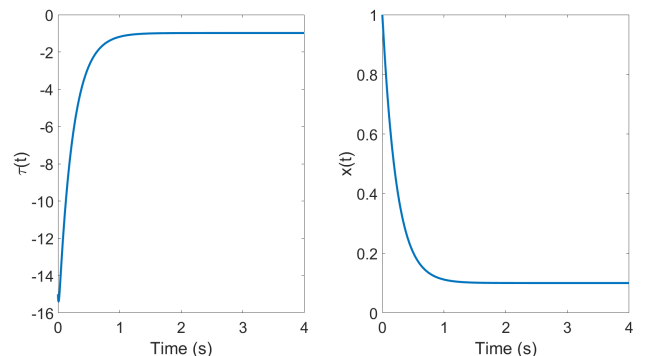


Fig. 9. Demonstrating simulation of box with friction example. The equilibrium is Lyapunov stable and the state trajectory, $x(t)$ does not reach origin because of stiction.

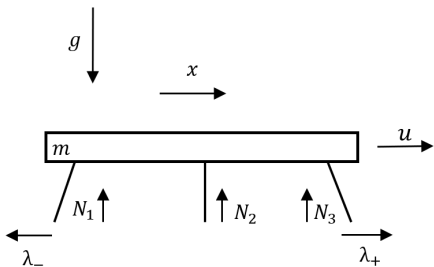


Fig. 10. Regulation task of a 3 legged table.

E. Three Legged Table

We examine a variation of Example D and consider a three legged table on a surface with Coulomb friction as in Figure 10. In this model, the coefficient of friction values (μ_1, μ_2, μ_3) are different for each leg of the table. The normal forces at the legs of the table are denoted by (N_1, N_2, N_3) and sum of the normal forces are equal to the mass times gravitational acceleration, mg . The net friction force is unique in static situations but it is non-unique during sliding since individual normal forces, N_i , are non-unique. The task is regulating the three legged table to the center. Newton's second law is approximated with a force balance equation with Coulomb friction and damping as in the previous example. Here, x is the position of the box, τ is the output of the low-pass filter, λ_+ is the positive component of the friction force, λ_- is the negative component of the friction force, γ is the slack variable, u is the force applied to the table:

$$\alpha \dot{x} = \tau + \lambda_+ - \lambda_-, \quad (25)$$

$$\dot{\tau} = \kappa(u - \tau), \quad (26)$$

$$0 \leq \gamma \perp \mu_1 N_1 + \mu_2 N_2 + \mu_3 N_3 - \lambda_+ - \lambda_- \geq 0, \quad (27)$$

$$0 \leq \lambda_+ \perp \gamma + \tau + \lambda_+ - \lambda_- \geq 0, \quad (28)$$

$$0 \leq \lambda_- \perp \gamma - \tau - \lambda_+ + \lambda_- \geq 0, \quad (29)$$

$$N_1 + N_2 + N_3 = mg, \quad (30)$$

$$N_1, N_2, N_3 \geq 0, \quad (31)$$

where $(\mu_1, \mu_2, \mu_3) = (0.1, 0.5, 1)$ are the coefficient of friction parameters for the legs of the table, $m = 1$ is the mass of the box, $g = 9.81$ is the gravitational acceleration, $\alpha = 4$ is the damping coefficient, and $\kappa = 100$ is the filter coefficient. The constraints (30) and (31) are exchanged with:

$$0 \leq N_1 \perp -mg + N_1 + N_2 + N_3 \geq 0,$$

$$0 \leq N_2 \perp -mg + N_1 + N_2 + N_3 \geq 0,$$

$$0 \leq N_3 \perp -mg + N_1 + N_2 + N_3 \geq 0,$$

to be consistent with the framework. We note that extending the framework to LCS models with additional equality and inequality constraints as in (25)-(31) is straightforward but it is omitted for brevity.

After using Algorithm 1, we find that $W = [0 \ 0 \ 0 \ 1 \ 1 \ 1]$. W shows that $N_1 + N_2 + N_3$ is unique, as expected since $N_1 + N_2 + N_3 = mg$. Note that $W\lambda = mg$ is a constant and the Lyapunov function (12) reduces to a common Lyapunov function. Based on the structure of W , unlike the previous

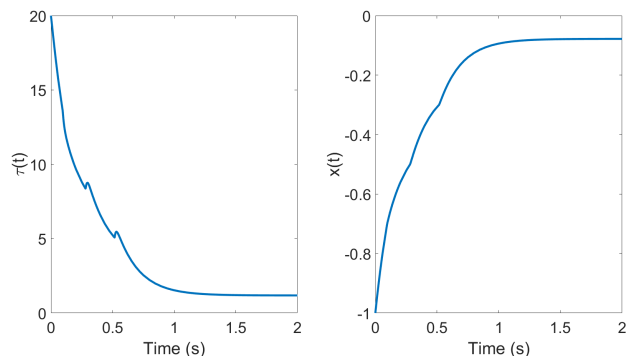


Fig. 11. Demonstrating simulation of three legged table example for the normal forces $N(t) = [4.0910, 4.1195, 1.5995]$ for $t \in [0, 0.2992)$, $N(t) = [5.4033, 3.1206, 1.2861]$ for $t \in [0.2992, 0.5455)$ and $N(t) = [9.4866, 0.1770, 0.1464]$ for $t \in [0.5455, \infty)$. The input u jumps at $t = 0.2992$ and $t = 0.5455$ but the force applied to system (τ) is continuous.

example, the net force $\lambda_+ - \lambda_-$ is not unique which is also expected due to the non-unique nature of normal forces. Notice that both the x -trajectory, $x(t)$ and λ -trajectory, $\lambda(t)$ are non-unique. We can solve the feasibility problem (24) in 19 seconds and find a controller of the form $u(x, \lambda) = Kx + L\lambda$ such that the origin is Lyapunov stable. The controller is not continuous in time since $L\lambda(t)$ term reacts directly to the measured forces, allowing feedback to function despite non-unique solutions.

In Figure 11, observe that the force applied to the system (τ) is continuous even though u is not, due to the low-pass filter. The origin is Lyapunov stable and the trajectory does not reach origin because of stiction.

F. 2D Simple Manipulation

We consider a quasi-static model of a box on a surface with friction parameter μ and two robotic arms that can interact with the box as in Figure 12. Similar to the previous example, we use the force balance equation with Coulomb friction and damping to model the dynamics of the box. The velocity of the manipulators can be controlled directly with delayed inputs τ_1 and τ_2 . In this model x_1, x_2, x_3 represent the positions of the box, the left manipulator and the right manipulator respectively. The contact forces λ_1 and λ_2 are non-zero if and only if the distance between the manipulators and the box is less than some threshold. We model the friction force with a positive component λ_+ and a negative component

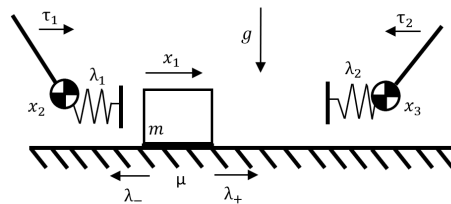


Fig. 12. 2D manipulation task where the goal is to regulate the position of the box on a surface with friction.

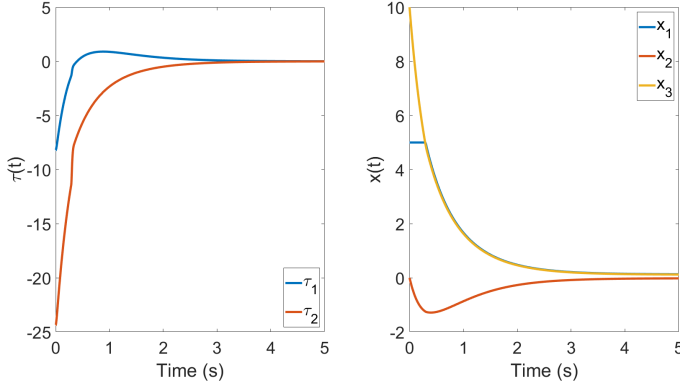


Fig. 13. Simulation results for 2D simple manipulation example. The forces applied to the box (τ) are smooth even though u is not, due to the low-pass filter model.

λ_- . In addition to that, we assume that we can not observe anything related to the box except the contact force between the manipulators and the box. The task is to regulate the box to the origin. We use the following model:

$$\begin{aligned} \alpha \dot{x}_1 &= \lambda_1 - \lambda_2 + \lambda_+ - \lambda_-, \\ \dot{x}_2 &= \tau_1, \\ \dot{x}_3 &= \tau_2, \\ \dot{\tau}_1 &= \kappa(u_1 - \tau_1), \\ \dot{\tau}_2 &= \kappa(u_2 - \tau_2), \\ 0 &\leq \lambda_1 \perp x_1 - x_2 + \frac{1}{k} \lambda_1 \geq 0, \\ 0 &\leq \lambda_2 \perp x_3 - x_1 + \frac{1}{k} \lambda_2 \geq 0, \\ 0 &\leq \gamma \perp \mu mg - \lambda_+ - \lambda_- \geq 0, \\ 0 &\leq \lambda_+ \perp \gamma + \lambda_1 - \lambda_2 + \lambda_+ - \lambda_- \geq 0, \\ 0 &\leq \lambda_- \perp \gamma - \lambda_1 + \lambda_2 - \lambda_+ + \lambda_- \geq 0, \end{aligned}$$

where $\kappa = 100$, $\mu = 0.1$, $m = 1$, $g = 9.81$, $\alpha = 1$, and $k = 100$. Since, F is not a P-matrix, we use Algorithm 1 and obtain

$$W = \begin{bmatrix} 1 & 0 & 0 & 0 & 0 \\ 0 & 1 & 0 & 0 & 0 \\ 0 & 0 & 0 & 1 & -1 \end{bmatrix}.$$

Observing W , the net friction force, $\lambda_+ - \lambda_-$, is unique. The contact forces between the manipulators and the box, λ_1, λ_2 are also unique.

Then we solve the optimization problem to find a controller that asymptotically stabilizes the system to a small ball around the origin $\mathcal{B} = \{x : x^T x \leq 0.1\}$. The optimization problem finds a result in 7.06 minutes and we obtain a controller of the form $u(x, \lambda) = Kx + L\lambda$ that stabilizes the system. This example shows that the contact-aware policy can be used for systems with non-unique contact forces, e.g., quasi-static friction, where we do not have full state information. In Figure 13, we demonstrate the performance of the controller.

G. Four Carts

As our last example, we consider the system in Figure 14. Here, (x_i, y_i) gives the position of the cart i . We approximate

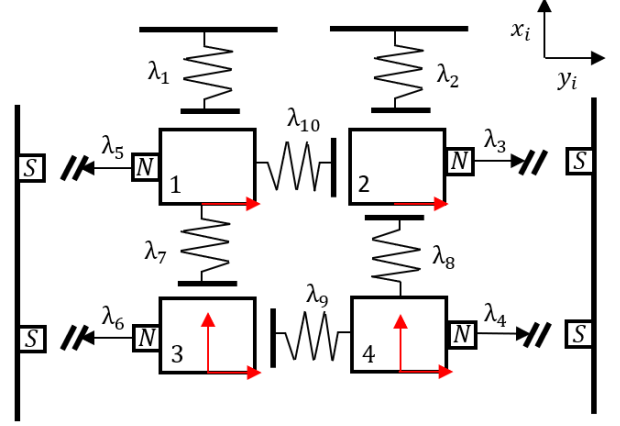


Fig. 14. Four carts example. The inputs that are applied to carts are represented by the red arrows.

Newton's second law with a force balance equation for each cart. The contact forces $\lambda_1, \lambda_2, \lambda_7, \lambda_8, \lambda_9$ and λ_{10} are soft contacts that are represented by the springs and are non-zero if the objects are closer than a threshold. The forces $\lambda_3, \lambda_4, \lambda_5$ and λ_6 approximate attractive magnetic forces between the carts and the walls and similarly are non-zero if the distance between the carts and the walls is less than a threshold. The red arrows represent the input forces that can be applied to carts. We model this system with $n = 8$ states, and $m = 10$ contacts where our goal is to show the performance of the proposed method on a high dimensional under-actuated example that is unstable without any control action. The model parameters are $A = 0_{8 \times 8}$, $c = 0_{10 \times 1}$, $F = I_{10 \times 10}$,

$$B = \begin{bmatrix} \begin{pmatrix} 1 & 0 \\ 0 & 0 \\ 0 & 1 \\ 0 & 0 \end{pmatrix} & 0_{4 \times 3} \\ 0_{3 \times 4} & I_{3 \times 3} \end{bmatrix},$$

$$D = \begin{bmatrix} 0 & 0 & 0 & 0 & -1 & 0 & 0 & 0 & 0 & -1 \\ -1 & 0 & 0 & 0 & 0 & 0 & 1 & 0 & 0 & 0 \\ 0 & 0 & 1 & 0 & 0 & 0 & 0 & 0 & 0 & 1 \\ 0 & -1 & 0 & 0 & 0 & 0 & 0 & 1 & 0 & 0 \\ 0 & 0 & 0 & 0 & 0 & -1 & 0 & 0 & -1 & 0 \\ 0 & 0 & 0 & 0 & 0 & 0 & -1 & 0 & 0 & 0 \\ 0 & 0 & 0 & 1 & 0 & 0 & 0 & 0 & 1 & 0 \\ 0 & 0 & 0 & 0 & 0 & 0 & 0 & -1 & 0 & 0 \end{bmatrix},$$

$$E = \begin{bmatrix} 0 & -1 & 0 & 0 & 0 & 0 & 0 & 0 \\ 0 & 0 & 0 & -1 & 0 & 0 & 0 & 0 \\ 0 & 0 & -1 & 0 & 0 & 0 & 0 & 0 \\ 0 & 0 & 0 & 0 & 0 & 0 & -1 & 0 \\ 1 & 0 & 0 & 0 & 0 & 0 & 0 & 0 \\ 0 & 0 & 0 & 0 & 1 & 0 & 0 & 0 \\ 0 & 1 & 0 & 0 & 0 & -1 & 0 & 0 \\ 0 & 0 & 0 & 1 & 0 & 0 & 0 & -1 \\ 0 & 0 & 0 & 0 & -1 & 0 & 1 & 0 \\ -1 & 0 & 1 & 0 & 0 & 0 & 0 & 0 \end{bmatrix}.$$

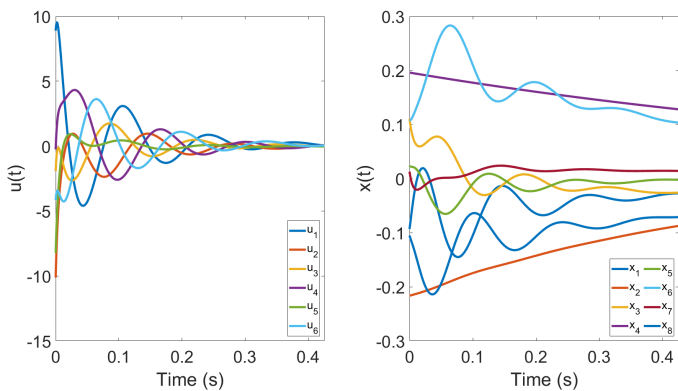


Fig. 15. Simulation of four carts example. The state trajectory, $x(t)$, asymptotically converges to the origin.

We can find a controller of the form $u(x, \lambda) = Kx + L\lambda$ that stabilizes the system. For this example, and higher dimensional examples in general, the initialization of the K and L matrices have a significant affect on the success of the algorithm. For this example, we initialized elements of K with sampling from uniform distribution ($K_{ij} \sim U[-100, 0]$). For one successful case, the algorithm terminates in 6 minutes and 58 seconds, but we also needed to run the algorithm approximately 20 hours with random seeds to obtain a successful result. In Figure 15, we present the performance of the controller.

VII. CONCLUSION

In this work, we have introduced a controller that can utilize both state and force feedback. We have demonstrated that combining linear complementarity systems with such tactile feedback controllers might result in an algebraic loop, and discussed how one can break such algebraic loops.

We have proposed an algorithm for synthesizing contact-aware control policies for linear complementarity systems with possibly non-unique solutions. For soft contact models, we have shown that pure local, linear analysis was entirely insufficient and utilizing contact in the control design is critical to achieve high performance. For systems with non-unique solutions, we have proposed a polynomial optimization program that can find matrices that map non-unique contact forces into a unique value, and used such mappings in our controller design algorithm. We have shown the effectiveness of our method on quasi-static friction models.

Furthermore, the proposed algorithm exploits the complementarity structure of the system and avoids enumerating the exponential number of potential modes, enabling efficient design of multi-contact control policies. Towards this direction, we have presented an example with eight states and ten contacts. In addition to incorporating tactile sensing into dynamic feedback, we provide stability guarantees for our design method.

The algorithm requires solving feasibility problems that include bilinear matrix inequalities and we have used PENBMI [49]. For the examples presented here, except the last one, the runtime of the algorithm was short and we found solutions to

the problems relatively quickly. On the other hand, it is important to note that for some parameter choices and initializations, the solver was unable to produce feasible solutions.

Interesting future work in this area will be using the controller presented here in physical experiments. We consider a hierarchical control framework where the tactile feedback policy is the higher level controller working together with a lower level controller to achieve a specified task. In addition, we intend to extend these algorithms to more complex tasks. For example, quasi-static models [17] where the matrix F depends on the generalized coordinates q . Another direction is designing controllers for systems where there are bilinear terms ($x_i \lambda_j$) in the dynamics, since we believe that bilinear terms are important when locally approximating a certain class of non-smooth systems.

REFERENCES

- [1] Y. Tassa and E. Todorov, "Stochastic Complementarity for Local Control of Discontinuous Dynamics," in *Proceedings of Robotics: Science and Systems (RSS)*, Citeseer, 2010.
- [2] F. R. Hogan, E. R. Grau, and A. Rodriguez, "Reactive Planar Manipulation with Convex Hybrid MPC," Oct 2017.
- [3] T. Marcucci, R. Deits, M. Gabbicini, A. Bicchi, and R. Tedrake, "Approximate Hybrid Model Predictive Control for Multi-contact Push Recovery in Complex Environments," in *2017 IEEE-RAS 17th International Conference on Humanoid Robotics (Humanoids)*, pp. 31–38, IEEE, 2017.
- [4] S. Sadraiddini and R. Tedrake, "Sampling-based Polytopic Trees for Approximate Optimal Control of Piecewise Affine Systems," in *2019 International Conference on Robotics and Automation (ICRA)*, pp. 7690–7696, IEEE, 2019.
- [5] M. Posa, M. Tobenkin, and R. Tedrake, "Stability Analysis and Control of Rigid-body Systems with Impacts and Friction," *IEEE Transactions on Automatic Control*, vol. 61, no. 6, pp. 1423–1437, 2015.
- [6] N. Wettels, J. Fishel, Z. Su, C. Lin, and G. Loeb, "Multi-modal Synergistic Tactile Sensing," in *Tactile Sensing in Humanoids - Tactile Sensors and Beyond Workshop, 9th IEEE-RAS International Conference on Humanoid Robots*, 2009.
- [7] J. W. Guggenheim, L. P. Jentoft, Y. Tenzer, and R. D. Howe, "Robust and Inexpensive Six-axis Force-torque Sensors Using MEMS Barometers," *IEEE/ASME Transactions on Mechatronics*, vol. 22, no. 2, pp. 838–844, 2017.
- [8] W. Yuan, R. Li, M. A. Srinivasan, and E. H. Adelson, "Measurement of Shear and Slip with a GelSight Tactile Sensor," in *2015 IEEE International Conference on Robotics and Automation (ICRA)*, pp. 304–311, IEEE, 2015.
- [9] V. Kumar, E. Todorov, and S. Levine, "Optimal Control with Learned Local Models: Application to Dexterous Manipulation," in *2016 IEEE International Conference on Robotics and Automation (ICRA)*, pp. 378–383, IEEE, 2016.
- [10] E. Donlon, S. Dong, M. Liu, J. Li, E. Adelson, and A. Rodriguez, "GelSlim: A High-Resolution, Compact, Robust, and Calibrated Tactile-sensing Finger," in *2018 IEEE/RSJ International Conference on Intelligent Robots and Systems (IROS)*, pp. 1927–1934, IEEE, 2018.
- [11] R. D. Howe, "Tactile Sensing and Control of Robotic Manipulation," *Advanced Robotics*, vol. 8, no. 3, pp. 245–261, 1993.
- [12] J. M. Romano, K. Hsiao, G. Niemeyer, S. Chitta, and K. J. Kuchenbecker, "Human-inspired Robotic Grasp Control with Tactile Sensing," *IEEE Transactions on Robotics*, vol. 27, no. 6, pp. 1067–1079, 2011.
- [13] A. Yamaguchi and C. G. Atkeson, "Combining Finger Vision and Optical Tactile Sensing: Reducing and Handling Errors While Cutting Vegetables," in *2016 IEEE-RAS 16th International Conference on Humanoid Robots (Humanoids)*, pp. 1045–1051, IEEE, 2016.
- [14] H. Merzic, M. Bogdanovic, D. Kappler, L. Righetti, and J. Bohg, "Leveraging Contact Forces for Learning to Grasp," *arXiv preprint arXiv:1809.07004*, 2018.
- [15] S. Tian, F. Ebert, D. Jayaraman, M. Mudigonda, C. Finn, R. Calandra, and S. Levine, "Manipulation by Feel: Touch-based Control with Deep Predictive Models," *arXiv preprint arXiv:1903.04128*, 2019.

- [16] M. K. Camlibel, J.-S. Pang, and J. Shen, "Lyapunov Stability of Complementarity and Extended Systems," *SIAM Journal on Optimization*, vol. 17, no. 4, pp. 1056–1101, 2006.
- [17] M. Halm and M. Posa, "A Quasi-static Model and Simulation Approach for Pushing, Grasping, and Jamming," *arXiv preprint arXiv:1902.03487*, 2019.
- [18] A. Aydinoglu, V. M. Preciado, and M. Posa, "Contact-aware Controller Design for Complementarity Systems," *To appear in ICRA 2020*.
- [19] R. Alur, T. A. Henzinger, G. Lafferriere, and G. J. Pappas, "Discrete Abstractions of Hybrid Systems," *Proceedings of the IEEE*, vol. 88, no. 7, pp. 971–984, 2000.
- [20] M. S. Branicky, V. S. Borkar, and S. K. Mitter, "A Unified Framework for Hybrid Control: Model and Optimal Control Theory," *IEEE Transactions on Automatic Control*, vol. 43, no. 1, pp. 31–45, 1998.
- [21] B. Brogliato, *Nonsmooth Mechanics*. Springer, 1999.
- [22] D. E. Stewart, "Rigid-body Dynamics with Friction and Impact," *SIAM review*, vol. 42, no. 1, pp. 3–39, 2000.
- [23] R. I. Leine and N. Van de Wouw, *Stability and Convergence of Mechanical Systems with Unilateral Constraints*, vol. 36. Springer Science & Business Media, 2007.
- [24] M. Anitescu and F. A. Potra, "Formulating Dynamic Multi-rigid-body Contact Problems with Friction as Solvable Linear Complementarity Problems," *Nonlinear Dynamics*, vol. 14, no. 3, pp. 231–247, 1997.
- [25] D. Stewart and J. C. Trinkle, "An Implicit Time-stepping Scheme for Rigid Body Dynamics with Coulomb Friction," in *Proceedings 2000 ICRA. Millennium Conference. IEEE International Conference on Robotics and Automation. Symposia Proceedings (Cat. No. 00CH37065)*, vol. 1, pp. 162–169, IEEE, 2000.
- [26] M. Posa, C. Cantu, and R. Tedrake, "A Direct Method for Trajectory Optimization of Rigid Bodies Through Contact," *The International Journal of Robotics Research*, vol. 33, no. 1, pp. 69–81, 2014.
- [27] M. Haas-Heger, G. Iyengar, and M. Ciocarlie, "On the Distinction Between Active and Passive Reaction in Grasp Stability Analysis," in *Workshop on the Algorithmic Foundation of Robotics (WAFR)*, 2016.
- [28] W. Heemels, J. M. Schumacher, and S. Weiland, "Linear Complementarity Systems," *SIAM Journal on Applied Mathematics*, vol. 60, no. 4, pp. 1234–1269, 2000.
- [29] D. Q. Mayne, "Control of Constrained Dynamic Systems," *European Journal of Control*, vol. 7, no. 2-3, pp. 87–99, 2001.
- [30] M. K. Camlibel *et al.*, "Complementarity Methods in the Analysis of Piecewise Linear Dynamical Systems," tech. rep., Tilburg University, School of Economics and Management, 2001.
- [31] H. Lin and P. J. Antsaklis, "Stability and Stabilizability of Switched Linear Systems: A Survey of Recent Results," *IEEE Transactions on Automatic Control*, vol. 54, no. 2, pp. 308–322, 2009.
- [32] R. W. Cottle, *Linear Complementarity Problem*. Springer, 2009.
- [33] J. Shen and J.-S. Pang, "Linear Complementarity Systems: Zeno States," *SIAM Journal on Control and Optimization*, vol. 44, no. 3, pp. 1040–1066, 2005.
- [34] P. A. Parrilo, "Semidefinite Programming Relaxations for Semialgebraic Problems," *Mathematical programming*, vol. 96, no. 2, pp. 293–320, 2003.
- [35] G. Stengle, "A Nullstellensatz and a Positivstellensatz in Semialgebraic Geometry," *Mathematische Annalen*, vol. 207, no. 2, pp. 87–97, 1974.
- [36] S. Boyd, L. El Ghaoui, E. Feron, and V. Balakrishnan, *Linear Matrix Inequalities in System and Control Theory*, vol. 15. SIAM, 1994.
- [37] M. A. Posa, T. Koolen, and R. L. Tedrake, "Balancing and Step Recovery Capturability via Sums-of-Squares Optimization," 2017.
- [38] M. Camlibel, W. Heemels, A. van der Schaft, and J. Schumacher, "Solution Concepts for Hybrid Dynamical Systems," in *IFAC World Congress*, 2002.
- [39] D. E. Stewart, *Rigid-Body Dynamics with Friction and Impact*, vol. 42. Jan 2000.
- [40] M. Halm and M. Posa, "Modeling and Analysis of Non-unique Behaviors in Multiple Frictional Impacts," in *Robotics: Science and Systems*, 2019.
- [41] G. V. Smirnov, *Introduction to the Theory of Differential Inclusions*, vol. 41. American Mathematical Soc., 2002.
- [42] H. K. Khalil, "Nonlinear Systems," *Upper Saddle River*, 2002.
- [43] M. Johansson and A. Rantzer, "Computation of Piecewise Quadratic Lyapunov Functions for Hybrid Systems," in *1997 European Control Conference (ECC)*, pp. 2005–2010, IEEE, 1997.
- [44] A. Mosek, "The MOSEK Optimization Software," *Online at <http://www.mosek.com>*, vol. 54, no. 2-1, p. 5, 2010.
- [45] J. F. Sturm, "Using SeDuMi 1.02, A MATLAB Toolbox for Optimization over Symmetric Cones," *Optimization Methods and Software*, vol. 11, no. 1-4, pp. 625–653, 1999.
- [46] A. Papachristodoulou and S. Prajna, "Robust Stability Analysis of Nonlinear Hybrid Systems," *IEEE Transactions on Automatic Control*, vol. 54, pp. 1035–1041, May 2009.
- [47] T. Marcucci and R. Tedrake, "Warm Start of Mixed-Integer Programs for Model Predictive Control of Hybrid Systems," *IEEE Transactions on Automatic Control*, 2020.
- [48] J. Löfberg, "YALMIP : A Toolbox for Modeling and Optimization in MATLAB," in *In Proceedings of the CACSD Conference*, (Taipei, Taiwan), 2004.
- [49] M. Kočvara and M. Stingl, "PENNON: A Code for Convex Nonlinear and Semidefinite Programming," *Optimization Methods and Software*, vol. 18, no. 3, pp. 317–333, 2003.
- [50] S. P. Dirkse and M. C. Ferris, "The PATH Solver: A Non-monotone Stabilization Scheme for Mixed Complementarity Problems," *Optimization Methods and Software*, vol. 5, no. 2, pp. 123–156, 1995.
- [51] R. Deits, T. Koolen, and R. Tedrake, "LVIS: Learning From Value Function Intervals for Contact-aware Robot Controllers," in *2019 International Conference on Robotics and Automation (ICRA)*, pp. 7762–7768, IEEE, 2019.
- [52] R. M. Murray and J. E. Hauser, *A Case Study in Approximate Linearization: The Acrobat Example*. 1991.